9th Asia-Pacific Conference on Wind Engineering
Auckland, New Zealand
3-7 December 2017

Analysis of Tornado-Induced Pressures and Internal Forces of a Building Frame

Changda Feng, Xinzhong Chen and Daan Liang

National Wind Institute, Department of Civil, Environmental and Construction Engineering, Texas Tech University, Lubbock, TX 79409, USA

Abstract

This study presents an analysis and characterization of dynamic tornado-induced pressures and internal forces of a low-rise building frame model using measurement data obtained from a tornado simulator. The time-varying mean and covariance of pressure are evaluated based on wavelet transform. The building frame responses are calculated from the statistics of pressures, and the equivalent static wind loads (ESWLs) causing peak responses are defined. The effect of translation speed of tornado vortex on frame responses is also explored. Finally, the tornado-induced responses are compared with those from ASCE 7-10.

Introduction

Tornados cause a great deal of damage on low-rise buildings. Tornado-induced pressures on low-rise buildings have different characteristics as compared to those under straight-line winds. A number of studies have explored the dynamic wind pressures and load effects on low-rise buildings under translating tornado-like vortices (e.g., [2,4-6]). This study presents an analysis of dynamic pressures and internal forces on a low-rise building frame using measurement data obtained from the tornado simulator at Iowa State University [2]. The deterministic time-varying mean pressure component is extracted from the time history record using discrete wavelet transformation (DWT) approach. The stochastic fluctuation component around the time-varying mean is then characterized in terms of time-varying standard variation (STD) and evolutionary power spectral density (EPSD) function, determined by a continuous wavelet transformation (CWT) based approach [3]. The analysis and characterization are also carried out for internal forces of building frame. The equivalent static wind loads (ESWLs) for tornado loading are proposed. The effect of translation speed of tornado vortex on frame responses is also explored. Finally, tornado-induced responses are compared with those determined using wind loads specified in ASCE 7-10.

Tornado-induced pressures on a building frame

Statistics of tornado-induced pressures

The simulated tornadoes had a swirl ratio of 0.08, a diameter to maximum wind speed of $D = 0.46$ m and a mean horizontal velocity at building height of $U_H = 8.3$ m/s. Two translation speeds of U_{TS} =0.15 and 0.61 m/s were considered. Each translation speed involved 10 repeated runs of measurements. The time scale was 1:13.8. The sampling frequency of pressure data was $f_s = 430$ Hz. The tornado-induced pressures were measured on a one-story gable roof building (length scale 1:100) with 91 mm by 91 mm plan and an eave height of 36 mm with the gable roof angle of 35° (figures.1 and 2). The surface pressures at 89 locations were simultaneously measured, which were denoted as $p_j(t) = 0.5\rho U_H^2 C_{pj}(t)$, where ρ is air density, and $C_{pj}(t)$ is pressure coefficient.

The dynamic pressure is modeled as a nonstationary random process with a deterministic time-varying mean and random fluctuation components. The time-varying mean component is considered to have frequencies lower than a pre-selected frequency, which is extracted by using DWT [3]. The cut-off frequency is 0.84 and 3.36 Hz respectively for the cases of translation speed $U_{TS} = 0.15$ and 0.61 m/s. Figure 3 shows an example of extraction of time-varying mean from pressure coefficient of Taps #3 at $U_{TS} = 0.15$ m/s. The time-varying character is plotted with respect to nondimensional distance x/D instead of time t, where x is distance from the center of tornado vortex to the center of building model.

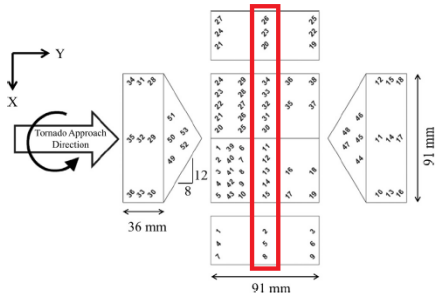

Figure 1. Layout and dimensions of building model

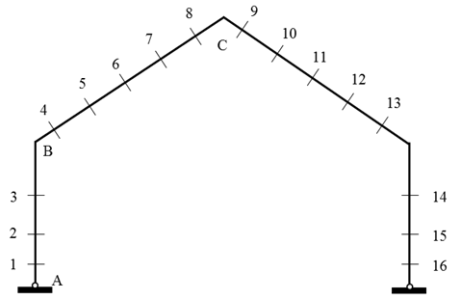

Figure 2. Building frame and pressure tap locations

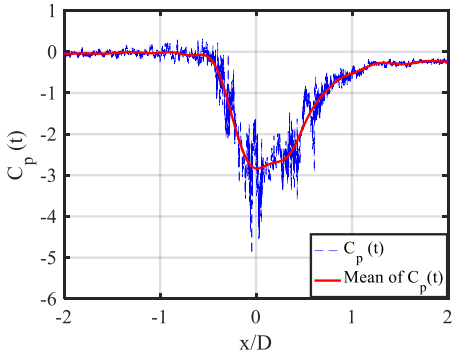

Figure 3. Examples of extraction of time-varying mean pressure coefficient of Tap #3 ($U_{TS} = 0.15$ m/s)

The CWT provides the wavelet coefficients of different scales at same time instants, thus facilitates estimations of EPSD and cross EPSD functions of nonstationary processes [3,7]. To reduce

the time variation of EPSD resulted from limited number of samples, moving average is also performed to smooth CWT coefficients before estimating EPSD. The window size of moving average in terms of non-dimensional distance x/D is 0.03. Once EPSD and cross EPSD are estimated, the time-varying variance and co-variance or correlation coefficient of the processes are determined. Figure 4 shows the time-varying STD of Tap #3 which is calculated through the integration of EPSD over the frequencies. The time-varying STD directly estimated from 10 time history samples at each time instant is also shown, where same moving average was also applied to smooth the time variation. It is observed that the estimated STD directly from the sample has larger variation due to limited number of samples available. The largest STD is observed around x/D=-0.25.

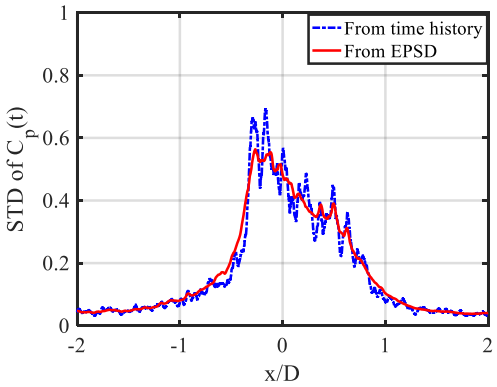

Figure 4. Time-varying STD estimated from EPSD and directly from time history of Tap #3 ($U_{TS} = 0.15$ m/s)

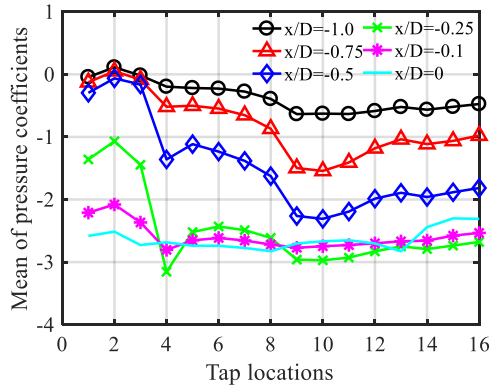

a) Mean pressure distribution

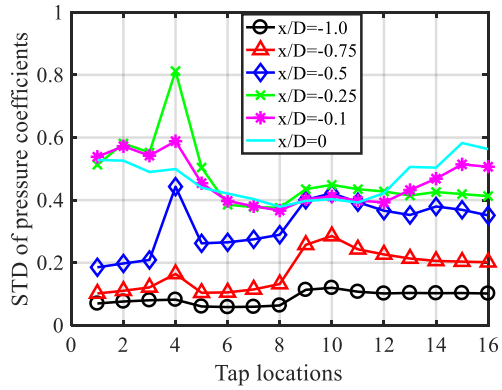

b) STD pressure distribution

Figure 5. Spatial variations of mean and STD pressure coefficients ($U_{TS} = 0.15$ m/s)

Spatial variation of pressure coefficients

Figure 5 shows the distributions of mean and STD of pressure coefficients on the building frame at different time instants, i.e., different locations of tornado x/D. As expected, the pressure distributions are strongly affected by the location of tornado. When the tornado vortex approaches, both mean and STD of pressure coefficients increase in their magnitudes. When the building frame is inside of tornado core, i.e., $|x|/D < 0.25$, the mean and STD of pressure coefficients tend to be more uniformly distributed due to the effect of pressure drop caused by tornado vortex. The lowest negative mean pressure coefficients for all pressure taps are around -2.8, which are consistent with the lowest mean ground-plane pressure coefficient of same simulated tornado without building [2]. The mean pressure coefficients on left wall (Taps #1-3) keep almost constant when $-1 < x/D < -0.5$, and then increase in magnitudes when tornado approaches. The mean pressure coefficients at other locations monotonically increase in magnitudes with the approaching of tornado vortex. The anti-symmetry property about $x/D = 0$ can be found for mean and STD of pressure distributions, thus these pressure distributions on $x/D > 0$ are not shown.

Building frame response

Characteristics of building frame response

The wind-induced response of the building frame at the building center is calculated using the pressure measurements. The building frame has pin-pin supports with rigid connections of column to beam and at top of the roof as shown in figure 2. The frame response in terms of axial force, shear force and bending moment at various sections can be calculated by using quasi-static analysis:

$$r(t) = \sum_{j=1}^{N} \mu_j A_j p_j(t) \quad (1)$$

where μ_j is influence coefficient representing the response r under unit static load at location z_j; $p_j(t)$ and A_j are pressure and tributary area at location z_j. The axial force, shear force and bending moment are normalized by dividing $0.5\rho U_H^2 BL$, $0.5\rho U_H^2 HL$ and $0.5\rho U_H^2 B^2 L$, where H, B and L are the frame height (6.6m), width (9.1m) and tributary length (4m). As the pressure distributions are almost symmetric with respect to the tornado location, only the responses at left half of the frame, i.e., sections A, B (on the roof) and C in figure 2, are addressed here. The positive directions of internal forces and moments are as follows: the axial force acts as a tensile force; the shear force causes a clockwise rotation of the frame segment on which it acts; the bending moment causes tension in the outside portion of fibers of the segment.

The time-varying mean and STD of the frame response can be determined in terms of time-varying mean and STD as well as covariance or correlation coefficients of wind loads:

$$\bar{r}(t) = \sum_{j=1}^{N} \mu_j A_j \bar{p}_j(t) \quad (2)$$

$$\sigma_r^2(t) = \sum_{i=1}^{N}\sum_{j=1}^{N} \mu_i \mu_j A_i A_j \rho_{ij}(t) \sigma_{p_i}(t) \sigma_{p_j}(t) \quad (3)$$

where $\bar{p}_j(t)$ and $\sigma_{p_j}(t)$ are time-varying mean and STD of $p_j(t)$; and $\rho_{ij}(t)$ is time-varying correlation coefficient between $p_i(t)$ and $p_j(t)$.

As an example, the time-varying mean and STD of internal forces at section B are shown in figure 6. Both axial force N_B and

shear force Q_B reach their maximum mean values at $x/D \approx -0.25$, while the maximum (absolute value) mean of bending moment M_B is observed at $x/D \approx -0.5$. Their maximum STDs are all observed at $x/D \approx -0.25$.

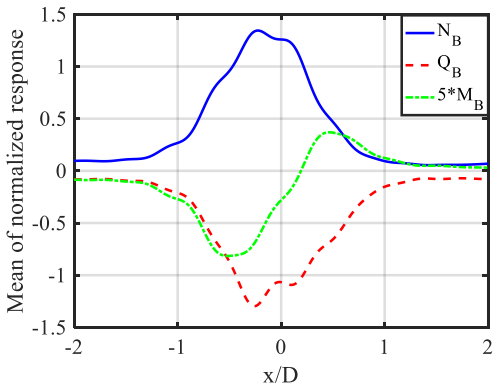

a) Mean

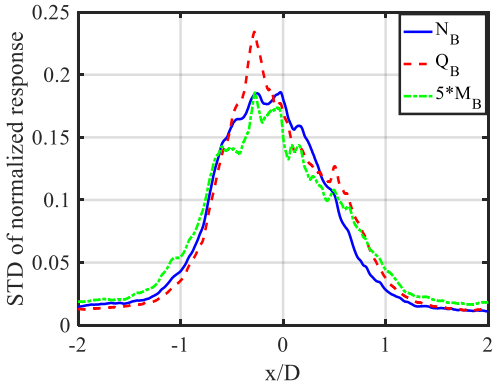

b) STD

Figure 6. An example of normalized internal forces of the frame ($U_{TS} = 0.15$ m/s)

Table 1 shows the maximums (absolute values) of mean and STD of the internal forces at $U_{TS} = 0.15$ m/s. The mean peak of internal forces calculated from the multiple time history samples is also presented. The peak factor and gust response factor (GRF) are then calculated as (mean peak –maximum mean)/maximum STD and mean peak/maximum mean, respectively. The mean component accounts for large part of peak response. The axial forces are all tension, and section A has the largest tension. The shear forces at sections B and C, Q_B and Q_C, are almost equal and both of them are larger than shear force at section A, Q_A. These large shear forces are caused by the suctions of the roof. The largest bending moment is observed at sections B. The peak factor is generally lower than that of stationary Gaussian process. The gust response factor is between 1.31-1.63.

In order to explore the translation effect on frame response, a similar analysis is made in the case of $U_{TS} = 0.61$ m/s, which is shown in table 2. The result shows the maximum mean responses are almost same at different translation speed. The maximum STD responses decrease with the increasing translation speed. The peak factor does not change a lot with different translation speeds. The gust response factors decrease with increasing translation speeds due to the reduction of response STDs. It is also noted that peak responses are not very sensitive to translation speed due to the less dynamic component compared with mean component. The translation speed is expected to have larger effect on fatigue damage of low-rise buildings due to the difference in loading cycles.

Table 1 Tornado load effects on frame at $U_{TS} = 0.15$ m/s (from samples)

	Max mean	Max STD	Peak	Peak factor	GRF	Peak from ESWLs (error %)
N_A	1.52	0.23	2.02	2.18	1.33	2.09 (3.1)
Q_A	-0.87	0.24	-1.29	1.75	1.48	-1.32 (2.1)
N_B	1.34	0.19	1.76	2.22	1.31	1.71(-2.6)
Q_B	-1.30	0.23	-1.91	2.62	1.46	-1.91 (0.2)
M_B	-0.16	0.04	-0.26	2.63	1.63	-0.26 (-0.5)
Q_C	1.36	0.21	1.94	2.76	1.43	1.64 (-15.6)
M_C	-0.09	0.02	-0.14	2.72	1.56	-0.05 (-60.7)
Total uplift	2.83	0.39	3.73	2.33	1.32	4.04 (8.2)
Total shear	-1.46	0.40	-2.17	1.76	1.49	-2.33 (7.6)

Table 2 Tornado load effects on frame at $U_{TS} = 0.61$ m/s (from samples)

	Max mean	Max STD	Peak	Peak factor	GRF	Peak from ESWLs (error %)
N_A	1.42	0.12	1.72	2.57	1.21	1.80 (4.3)
Q_A	-0.84	0.14	-1.13	2.05	1.34	-1.14 (0.9)
N_B	1.28	0.11	1.55	2.48	1.21	1.48 (-4.9)
Q_B	-1.20	0.11	-1.51	2.68	1.25	-1.65 (9.6)
M_B	-0.16	0.02	-0.22	2.26	1.35	-0.22 (3.9)
Q_C	1.34	0.15	1.64	2.08	1.23	1.38 (-16.4)
M_C	-0.08	0.01	-0.11	2.67	1.33	-0.05 (-57.5)
Total uplift	2.70	0.23	3.31	2.64	1.22	3.48 (5.2)
Total shear	-1.36	0.26	-1.78	1.64	1.31	-2.01 (13.1)

Modeling of equivalent static wind load

As shown in figure 6, the peaks of different responses occur at different locations of tornado vortex center, which correspond to different pressure distributions. In order to define convenient ESWLs for various peak responses under tornado loading, the gust response factor based modeling approach is adopted here, which defines the ESWLs as mean loads multiplied by gust response factors. The overall guest response factor is selected as 1.45 and 1.29 for U_{TS} =0.15 m/s and 0.61 m/s, respectively. The ESWLs in terms of pressure distributions are shown in figure 7 in the case of U_{TS} =0.15 m/s. These pressure distributions are developed based on mean pressure distributions at x/D=-0.5 and -0.25 and also take into account the gust response factors. Considering the approximate symmetry of pressure distribution with respect to the location of tornado center, other two corresponding ESWLs should also be used, which are given by simply flipping the distribution around the top of the roof. The maximum response under these four ESWLs are selected and the results are shown in tables 1 and 2 for U_{TS} =0.15 m/s and 0.61 m/s. The results show that the proposed ESWLs give accurate estimation of frame responses except M_C and Q_C. Q_C can be set to be the same magnitude of Q_B with opposite sign. The magnitude of M_C is very small and can be approximately set as same as M_B in design practice.

A different building frame with same geometric configuration but different structural system is also used to check the effectiveness of ESWLs. The frame has the same cross sections with previous one but with fix-fix supports and a hinge in the middle of roof, and is denoted as ‘‘New frame’’. Table 3 compares

the peak responses from time history samples and from ESWLs of new frame at different translation speeds. It shows that the ESWLs work well for all the responses for a different building frame. The result also shows that the ESWLs are not sensitive to structure system.

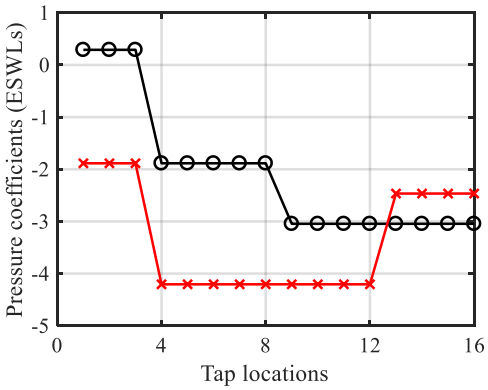

Figure 7. ESWLs in terms of pressure distribution for calculating maximum responses

Table 3 Comparison of peak responses of the new frame from samples and ESWLs (error %)

	U_{TS} = 0.15 m/s		U_{TS} = 0.61 m/s	
	Samples	ESWLs	Samples	ESWLs
N_A	1.93	2.08 (7.6)	1.66	1.79 (8.2)
Q_A	-1.51	-1.41 (-6.2)	-1.29	-1.22 (-5.6)
M_A	-0.14	-0.14 (-1.5)	-0.13	-0.12 (-3.1)
N_B	1.53	1.65 (7.5)	1.39	1.42 (2.7)
Q_B	-1.90	-1.97 (3.6)	-1.53	-1.70 (10.7)
M_B	-0.12	-0.11 (-12.6)	-0.10	-0.09 (-11.8)
Q_C	1.63	1.54 (-5.5)	1.37	1.33 (-2.7)

Table 4 Comparison of peak responses based on ASCE 7-10

	Original frame		New frame	
Response	ASCE 7-10	Ratio	ASCE 7-10	Ratio
N_A	0.50	4.1	0.34	5.7
Q_A	0.98	1.3	1.04	1.5
M_A	-	-	0.12	1.2
N_B	0.38	4.7	0.33	4.6
Q_B	-0.48	4.0	-0.26	7.4
M_B	-0.17	1.5	-0.06	2.0
Q_C	-0.62	3.1	-0.33	4.9
M_C	0.02	8.5	-	-
Total uplift	0.63	5.9	0.63	5.9
Total shear	1.76	1.2	1.76	1.2

Comparison with ASCE 7-10

The wind-induced responses of same frames are also calculated based on wind loads specified in ASCE 7-10 [1]. The mean horizontal velocity at building height U_H=8.3 m/s in tornado simulator is transferred to $U_{10} = 8.3(10/6.6)^{1/6.5}$=8.8 m/s at the height of 10 m Explore C in ASCE 7-10. The velocity data is averaged in 26 s in simulator, which is 6-min in full scale. The 6-min mean wind speed converts to 3s-gust wind speed in ASCE 7-10 by multiplying a factor of 1.39. For ASCE 7-10 wind loads, $K_z = 0.85$, K_d and K_{zt} are taken as 1. The wind pressure coefficients are used as MWFRS of "All height method" in Chapter 27 of ASCE 7-10. Table 4 gives responses from ASCE 7-10 wind loads, and the ratios of tornado peak responses (U_{TS}=0.15 m/s) to ASCE responses for both original and new frames. It is observed that the response from ASCE 7-10 are much lower compared with that of tornado loads, which is primarily attributed to the large suctions on the roof caused by tornado vortex. The total uplift under tornado load is 6 times of that under ASCE 7-10, while the total shears of both cases are almost the same.

Conclusions

The dynamic wind pressures and integrated forces on a low-rise building model under tornado vortex were analyzed. Wavelet transform tools were used to determine time-varying mean and STD of pressures. The pressure distributions are strongly affected by tornado locations and are tend to be more uniformly distributed when building frame is inside of tornado core. As the result, the building frame responses are much larger than those estimated using the wind load specified in ASCE7-10. The ESWLs of tornado loading defined based on gust response factor approach gave reasonably accurate estimation of tornado-induced peak responses. The maximum mean responses and peak factors are not sensitive to translation speed. The gust response factor and peak response decrease with increasing translation speed due to the reduce of response STD.

Acknowledgments

The support for this work provided in part by NSF grant No. CMMI-1400224 and CMMI-1536108 is greatly acknowledged. The writers would like to express their appreciations to Prof. Partha Sarkar from Iowa State University for his valuation comments and contributions.

References

[1] ASCE 7-10 (2011). Minimum design loads for buildings and other structures. ASCE, Reston, VA, USA.

[2] Haan Jr, F.L., Balaramudu, V.K. and Sarkar, P.P. (2010). Tornado-induced wind loads on a low-rise building. J. Struct. Eng., 136(1), 106-116.

[3] Huang, G. and Chen, X. (2009). Wavelets-based estimation of multivariate evolutionary spectra and its application to nonstationary downburst winds. Eng. Struct., 31(4), 976-989.

[4] Kumar, N., Dayal, V. and Sarkar, P. P. (2012). Failure of wood-framed low-rise buildings under tornado wind loads. Eng. Struct., 39, 79-88.

[5] Roueche, D. B., Prevatt, D. O., Haan, F. L. and Datin, P. L. (2015). An estimate of tornado loads on a wood-frame building using database-assisted design methodology. J. Wind Eng. Ind. Aerodyn., 138, 27-35.

[6] Sengupta, A., Haan, F. L., Sarkar, P. P. and Balaramudu, V. (2008). Transient loads on buildings in microburst and tornado winds. J. Wind Eng. Ind. Aerodyn., 96(10), 2173-2187.

[7] Spanos, P. D. and Failla, G. (2004). Evolutionary spectra estimation using wavelets. J. Eng. Mech., 130(8), 952-960.